Environ Sci Pollut Res (2016) 23:1158–1172
DOI 10.1007/s11356-015-5648-3

RESEARCH ARTICLE

Characteristics of ammonia, acid gases, and $PM_{2.5}$ for three typical land-use types in the North China Plain

Wen Xu[1] · Qinghua Wu[1] · Xuejun Liu[1] · Aohan Tang[1] · Anthony J. Dore[2] · Mathew R. Heal[3]

Received: 18 April 2015 / Accepted: 19 October 2015 / Published online: 27 October 2015

Abstract Air pollution is one of the most serious environmental problems in China due to its rapid economic development alongside a very large consumption of fossil fuel, particularly in the North China Plain (NCP). During the period 2011–2014, we integrated active and passive sampling methods to perform continuous measurements of NH_3, HNO_3, NO_2, and $PM_{2.5}$ at two urban, one suburban, and two rural sites in the NCP. The annual average concentrations of NH_3, NO_2, and HNO_3 across the five sites were in the ranges 8.5–23.0, 22.2–50.5, and 5.5–9.7 μg m^{-3}, respectively, showing no significant spatial differences for NH_3 and HNO_3 but significantly higher NO_2 concentration at the urban sites. At each site, annual average concentrations of NH_3 and NO_2 showed increasing and decreasing trends, respectively, while there was no obvious trend in annual HNO_3 concentrations. Daily $PM_{2.5}$ concentrations ranged from 11.8 to 621.0 μg m^{-3} at the urban site, from 19.8 to 692.9 μg m^{-3} at the suburban site, and from 23.9 to 754.5 μg m^{-3} at the two rural sites, with more than 70 % of sampling days exceeding 75 μg m^{-3}. Concentrations of water-soluble ions in $PM_{2.5}$ ranked differently between the non-rural and rural sites. The three dominant ions were NH_4^+, NO_3^-, and SO_4^{2-} and mainly existed as $(NH_4)_2SO_4$, NH_4HSO_4, and NH_4NO_3, and their concentrations averaged 48.6±44.9, 41.2±40.8, and 49.6±35.9 μg m^{-3} at the urban, suburban, and rural sites, respectively. Ion balance calculations indicated that $PM_{2.5}$ was neutral at the non-rural sites but acidic at the rural sites. Seasonal variations of the gases and aerosols exhibited different patterns, depending on source emission strength and meteorological conditions. Our results suggest that a feasible pathway to control $PM_{2.5}$ pollution in the NCP should target ammonia and acid gases together.

Keywords Air pollution · Reactive N · $PM_{2.5}$ · Control strategies · Chemical characteristics · The North China Plain

Responsible editor: Philippe Garrigues

Electronic supplementary material The online version of this article (doi:10.1007/s11356-015-5648-3) contains supplementary material, which is available to authorized users.

✉ Xuejun Liu
liu310@cau.edu.cn

[1] College of Resources and Environmental Sciences, China Agricultural University, Beijing 100193, China

[2] Centre for Ecology and Hydrology, Edinburgh, Bush Estate, Penicuik, Midlothian EH26 0QB, UK

[3] School of Chemistry, The University of Edinburgh, David Brewster Road, Edinburgh EH9 3FJ, UK

Introduction

In China, the atmospheric environment has been greatly affected over recent decades by various anthropogenic factors, such as a dramatic economic rise, rapid industrial development, population growth, and construction and demolition projects. The increase of traffic flow is also of central importance. As a consequence, complex air pollution events characterized by regional photochemical smog and haze occur frequently in many regions of China (Wang et al. 2014a), arousing increasing attention from the private citizen as well as environmental scientists and policy makers. The smog and haze largely result from high levels of particulate matter (PM), especially $PM_{2.5}$ (particular matter less than 2.5 μm), which limits atmospheric visibility by light extinction (absorption and scattering) (Sun et al. 2006; Wang et al. 2012a). Several studies focusing on health effects have revealed associations between PM pollution and morbidity and mortality, including

in the USA (Doninici et al. 2014) and China (Guo et al. 2009; Wu et al. 2010). It has been estimated that 350,000–400,000 premature deaths can be ascribed to ambient air pollution in China, and the economic burden of premature mortality and morbidity was conservatively estimated at approximately 157 billion RMB (1.16 % of the GDP) in 2003 (Zhang and Smith 2007; WB 2007).

Airborne $PM_{2.5}$ can be directly emitted by anthropogenic sources or generated by gas-to-particle conversion (secondary PM) (Watson 2002). The primary precursors for formation of ammonium sulfate (or bisulfate) and ammonium nitrate are NH_3, SO_2, and NO_x ($NO+NO_2$). Atmospheric NH_3 is emitted primarily from livestock wastes and volatilization of N fertilizers. Other sources include biomass burning, excreta of human and pets, and wastewater (Clarisse et al. 2009). NO_x and SO_2 are mainly derived from combustion processes and are subsequently oxidized to HNO_3 and H_2SO_4 in the atmosphere (Sharma et al. 2007).

In order to prevent further deterioration of air quality, China has made tremendous efforts since 2005. For example, the 11th Five-Year Plan (FYP) (2006–2010) for national environmental protection required the reduction of annual SO_2 emissions in 2010 by 10 % from its 2005 level, which required installation of flue-gas desulfurization systems to coal-fired power plants as a primary control measure and a stronger vehicle emissions standard. As a consequence, national SO_2 emissions decreased by 14.3 % from 2005 to 2010 (MEPC 2011). In the 12th FYP (2011–2015), China is mainly focused on the reduction of national NO_x emissions by 10 % in 2015 from the 2010 level, as well as controls on SO_2 and primary particle emissions. To achieve this binding target, China's Ministry of Environmental Protection (MEP) released a new "emission standard of air pollutants for thermal power plants" (GB 13223-2011) in 2011 to further strengthen the NO_x controls. Furthermore, a stricter vehicle emissions standard (equivalent to the European Union's Euro IV standard) was also released in late 2012. Unfortunately, legislation to simultaneously reduce NH_3 emissions has not been implemented in China. Such legislation is urgently needed given that the estimated health costs associated with NH_3 emissions were greater than those associated with NO_x emissions in more than 77 % of provinces in China, particularly in the North China Plain (NCP) (Gu et al. 2014).

The NCP is an intensively managed agricultural and economically developed region, which comprises only 8 % of the total area of China but contributes 40 % of the total national GDP (CSY 2014). The consumption of N fertilizer and energy in the NCP accounted for 35 and 34 % of their respective total national consumption (CSY 2014). This makes the NCP one of the greatest emitters of air pollutants (e.g., NH_3, NO_x, and SO_2) nationally and globally (Clarisse et al. 2009; Zhang et al. 2009; Gu et al. 2012; Huang et al. 2012) and a serious $PM_{2.5}$ pollution region in China (Wang et al. 2014b). Some studies have focused on the measurements of atmospheric NO_2 and NH_3 at various sites in the NCP (Shen et al. 2009, 2011; Meng et al. 2011; Pan et al. 2012; Luo et al. 2013) and on estimating of emissions of NO_2 and NH_3 from anthropogenic sources (Zhang et al. 2010, 2011b). Very few studies in the NCP have considered ambient HNO_3 measurements (Shen et al. 2009; Luo et al. 2013). $PM_{2.5}$ has been systematically analyzed in many studies in the NCP. Most of the studies have provided the general characteristics of the chemical compositions of $PM_{2.5}$ and discussed its seasonal variations, correlations, or sources (Sun et al. 2004; Song et al. 2006). Additionally, the concentration, correlations, sources, or formation of some specific species (e.g., inorganic ions, carbonaceous components, or organic matter) and their spatial variations have been investigated in the NCP (Ianniello et al. 2011; Zhao et al. 2013; Hu et al. 2014). However, few studies have measured NO_x, NH_3, HNO_3, and $PM_{2.5}$ simultaneously. In addition, previous work has mainly included short-term studies before the year 2010 and has been limited to single land-use types (e.g., urban areas). In the absence of long-term and simultaneous observations, the characteristics of these air pollutants and their implications cannot be determined accurately.

In the present study, ambient NO_x, NH_3, and HNO_3 were continuously monitored at five typical sites (two urban, one suburban, and two rural) in the NCP during the period 2011–2014, and $PM_{2.5}$ was sampled at four of the five sites. The objectives of this study were (1) to characterize spatial, seasonal, and annual variations of concentrations for the measured gases and evaluate their pollution status during the period from 2011 to 2014 and (2) to analyze the concentrations and seasonal variations of $PM_{2.5}$ and its secondary inorganic components over different land-use types. The intention of the study was to provide accurate and current insight into the characteristics of air pollutants and to support interpretation of the effectiveness of major national control policies implemented recently in the NCP.

Materials and methods

Sampling sites

Sampling was conducted between January 2011 and December 2014 at five sites in Beijing and in Henan, Shandong, and Hebei provinces (Fig. 1), which are located in the North China Plain. The area has a typical temperate and monsoonal climate with dry winters and wet summers. The prevailing wind direction is from the southeast in the summer and northwest in the winter.

Two urban sites were at the China Agricultural University (CAU) and Zhengzhou (ZZ), a suburban site was at Shangzhuang (SZ), and two rural sites were at Quzhou (QZ) and Yucheng (YC). The CAU site is located at the west

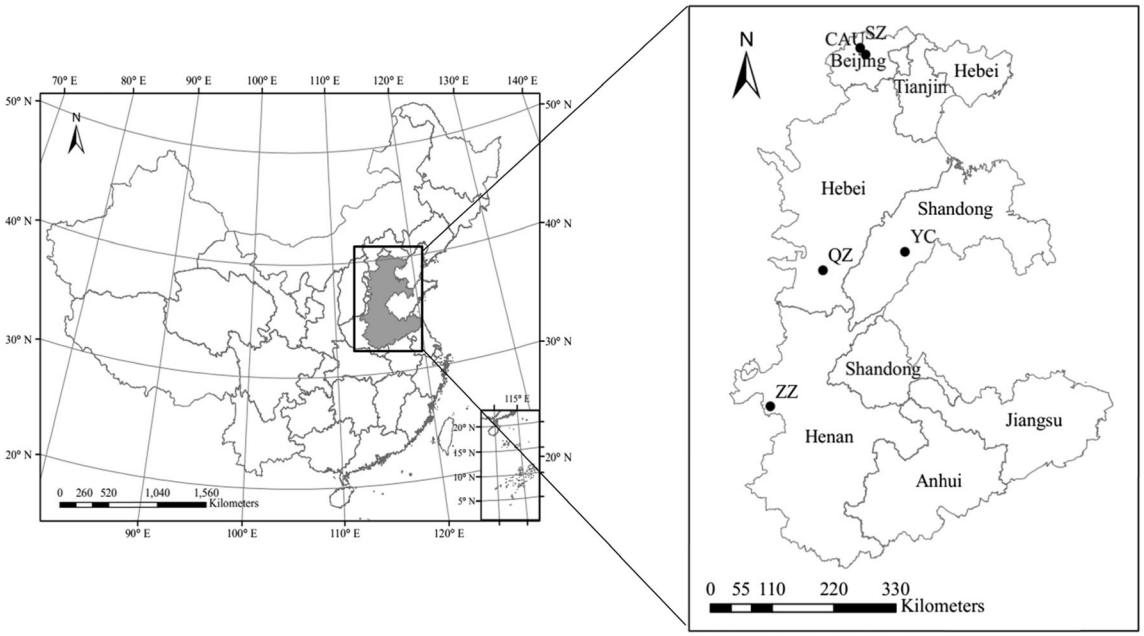

Fig. 1 Geographical distribution of the five sampling sites in the North China Plain: urban sites (CAU, ZZ), suburban site (SZ), and rural sites (QZ, YC)

campus of the China Agricultural University (40.02° N, 116.28° E, 55 m above sea level (m.a.s.l.)) which is situated in the northwestern urban area of Beijing. The ZZ site is located at Henan Academy of Agricultural Sciences (34.75 °N, 113.63 °E, 91 m.a.s.l.), which is in the center of Zhengzhou, the capital of Henan province. The SZ site is located at Shuangzhuang Agricultural Experimental Station (40.11° N, 116.20° E, 47 m.a.s.l.) in Shuangzhuang town, which is situated to the northwest of Beijing, about 33 km from the city center. Quzhou (QZ) is a typical rural agriculture dominated site with a recently constructed industrial district, about 60 km northeast of Handan city, Hebei province. The sampling site was located at Quzhou Agricultural Experimental Station (36.78° N, 114.94° E, 37 m.a.s.l.). The YC site is located at Yucheng Experimental Station (36.94° N, 116.63° E, 24 m.a.s.l.), Chinese Academy of Sciences, about 60 km southeast of Dezhou city, Shandong province. The measurement height and period, and other information on sampling sites such as measured species, possible emissions and density of population, are given in Table 1.

Sampling methods and chemical analysis

NH_3 and HNO_3 samples were collected using the DELTA (DEnuder for Long-Term Atmospheric sampling) system designed by the Centre for Ecology and Hydrology Edinburgh, UK. The DELTA system has been used widely in Europe and described in detail in many previous studies (e.g., Flechard et al. 2011; Luo et al. 2013; Shen et al. 2013). Briefly, the DELTA sampling "train" consists of two potassium carbonate plus glycerol (1 % (*m*/*v*) K_2CO_3+1 % (*m*/*v*) glycerol in methanol)-coated denuders in series for the simultaneous collection of HNO_3, followed by two citric acid (5 % (*m*/*v*) citric acid in methanol)-coated denuders for NH_3. A low-volume pump (D210, TCS Micropumps Ltd., UK) in the DELTA system was used to sample ambient air at a rate of 0.2–0.4 L min^{-1}. When the air passes through a denuder filter train, HNO_3 and NH_3 in the air are absorbed by the coated chemical solutions in sequence. With a monthly sampling period, the detection limit of the DELTA system for gaseous HNO_3 and NH_3 was determined as 0.03 μg $HNO_3 m^{-3}$ and 0.01 μg $NH_3 m^{-3}$. Two denuders in series are used for every sample to check capture efficiency for HNO_3 and NH_3. When the value is less than 75 %, an imperfectly coated film or some other sampling problems can be assumed to have occurred in the DELTA system (Tang et al. 2009). Across the five sites, collection efficiencies in the first of the two denuders for HNO_3 and NH_3 averaged 83.2 % (95 % confidence interval 81.5–84.9 %) and 82.7 % (81.3–84.1 %), respectively, during the entire period. Thus, we can be assured that both of measured gases were effectively captured in both denuders. It should be noted that nitrous acid (HONO) could cause a positive bias in the long-term measurement of HNO_3 using the DELTA system (Tang et al. 2009). This is of importance in urban areas whereas HONO interference (as well as possible NO_2 and PAN interference) should be negligible in rural areas. In this study, glycerol was added to the coating of the denuder for HNO_3 sampling in order to increase adhesion and reduce volatilization of the carbonate coating and also to minimize oxidation of nitrite to nitrate which can occur when ozone is present (Allegrini et al. 1987; Perrino et al. 1990; Tang et al. 2009). In addition, the average denuder capture efficiency for HNO_3 was 83.2 % in the first denuder as noted earlier, indicating little evidence of significant NO_2 or PAN capture (Tang

Table 1 Descriptions of the five monitoring sites and the corresponding measurements in this study

Monitoring site	Species	Monitoring period		Measurement height (m) and underlying surface			Population density (persons km^{-2})[b]	Surrounding environment and possible emission sources
		Gases[a]	$PM_{2.5}$	Gases	$PM_{2.5}$	Surface		
China Agricultural University (CAU)	NH_3, HNO_3, NO_2, $PM_{2.5}$	Jan. 2011–Dec. 2014	Mar. 12–Nov. 2014	2	10	Roof	7616	Densely occupied residences, small-scale urban agriculture, and traffic roads
Shangzhuang (SZ)	NH_3, HNO_3, NO_2, $PM_{2.5}$	Jan. 2011–Dec. 2014	Apr. 12–Nov. 2014	2	2.5	Grass	519	Small towns, traffic roads, and farmland
Quzhou (QZ)	NH_3, HNO_3, NO_2, $PM_{2.5}$	Jan. 2011–Dec. 2014	Apr. 12–Nov. 2014	2	2.5	Grass	606	Small villages, a traffic road, and dense farmland
Yucheng (YC)	NH_3, HNO_3, NO_2, $PM_{2.5}$	Jan. 2013–Dec. 2014	Apr. 13–Nov. 2014	2	2.5	Lawn	495	Small villages, a road, and farmland
Zhengzhou (ZZ)	NH_3, HNO_3, NO_2	Jan. 2011–Dec. 2014	n.d.	2	–	Grass	17,069	Densely occupied residences and traffic roads

n.d. not determined

[a] NH_3, HNO_3, and NO_2

[b] Population density was estimated by dividing population by area of the town/district/county where the monitoring site is located. Population data were sourced from the sixth census of China in 2010 (http://www.stats.gov.cn)

et al. 2009). Nevertheless, measured HNO_3 concentrations may be overestimated to some extent at the urban CAU site but could reflect actual levels at suburban and rural sites. In future work, HNO_3 should be selectively removed from the sampling air by first using a sodium fluoride or sodium fluoride-coated denuder as widely used in previous studies (Allegrini et al. 1987; Spataro et al. 2013). For NH_3 sampling, Perrino and Gherardi (1999) have highlighted that in the case of citric acid, about 8 % of the collected ammonia was released after 2 h and more than 40 % after 12 h. In contrast, phosphorous acid is a suitable coating layer for a denuder line intended to determine gaseous ammonia in the atmosphere (Perrino and Gherardi 1999). However, an intercomparison study conducted by Tang et al. (2009) showed that the 14-day mean NH_3 concentration from citric acid-coated denuders of a DELTA system was about 9 % lower than that from H_3PO_3-coated denuders of an Annular Denuder System. Given this, together with an overall 82.7 % NH_3 capture efficiency as noted earlier, NH_3 concentrations sampled at the five sites should be reasonable and acceptable, albeit with some degree of underestimation.

NO_2 samples were collected by Gradko diffusion tubes (Gradko International Limited, UK). Each sampler consists of a 71.0-mm long×11.0-mm internal diameter acrylic tube with colored and white thermoplastic rubber caps. Three NO_2 samplers at each site were exposed under a PVC shelter which protected the samplers from precipitation and direct sunshine. The NO_2 was absorbed into a 20 % triethanolamine/deionized water solution coated onto two stainless steel wire meshes within the colored cap. As indicated by the manufacturer (Gradko International Ltd, UK), the uptake rate of the tube is 68.8×10^{-6} m^{-3} h^{-1}, the desorption efficiency is 0.98, the limit of detection is 1.6 μg $NO_2 m^{-3}$ over a 2-week exposure period, and the analytical expanded measurement uncertainty is ±10 %. Over the entire period, the standard deviations of each sampling across all sites ranged from 0.01 to 2.9 μg NO_2 m^{-3} and averaged 0.8 μg $NO_2 m^{-3}$ (95 % confidence interval 0.7–0.9).

All the samplers were exposed for 1 month at each site and returned to the laboratory for analysis. In the laboratory, all the exposed samples were stored at 4 °C and analyzed at 1-month intervals. The HNO_3 denuders were extracted with 10 mL 0.05 % H_2O_2 solution. The NH_3 denuders were extracted with 10 mL high-purity water. Ammonium and nitrate in the extracted solutions were measured with an AA3 continuous-flow analyzer (Bran+Luebbe GmbH, Norderstedt, Germany). The detection limits were determined as 0.01 mg N L^{-1} for NH_4^+ and NO_3^-. The meshes from the NO_2 diffusion tubes were extracted with a solution containing sulfanilamide, H_3PO_4, and N-1-naphthylethylene-diamine, and the NO_2 content in the extract determined using a colorimetric method by absorption at a wavelength of 542 nm. The detection limit for NO_2 was 0.01 mg N L^{-1}. The laboratory and field blank

samples were extracted and analyzed using the same methods as the exposed samples. After correcting for the corresponding blanks, the results were used for the calculation of concentrations for all measured gases.

Samples of $PM_{2.5}$ were collected by medium-volume samplers (TH-150CIII, 100 L min^{-1}, Tianhong Co., Wuhan, China) onto 90-mm quartz fiber filters (Whatman QM/A, Maidstone, UK) at all sites except ZZ because only four particle samplers were available. The quartz fiber filters were baked at 500 °C for 4 h prior to sampling to remove contaminants. The $PM_{2.5}$ samples were collected on a 24 hourly basis from 08:00 hours to 08:00 hours the next day. More than 25 valid samples were obtained for most seasons during the sampling period at each site. Owing to precipitation or occasional sampler failure, a number of seasons have less than 20 samples.

Before and after sampling, the filters were equilibrated for 24 h in a desiccator at 25 °C and 40±5 % relative humidity and then weighed with a microbalance (Sartorius, precision 10 μg). The $PM_{2.5}$ concentrations were calculated by weight differences divided by sampling air flows. A quarter of each filter was put into a 50-mL beaker with 10 mL of high-purity water (18.2 MΩ resistivity). After a 30-min ultrasonic extraction, the extracts were filtered using 0.22-μm syringe filters, and the filtrates were stored in clean tubes at 4 °C until analyzed within 1 month of extraction. The cations (NH_4^+, Na^+, Ca^{2+}, K^+, Mg^{2+}) and anions (NO_3^-, SO_4^{2-}, F^-, Cl^-) in the filtrates were determined by Dionex-600 and Dionex-2100 Ion Chromatograph (Dionex Inc., Sunnyvale, CA, USA), respectively. Details of the instruments and detection limits have been provided elsewhere (Zhang et al. 2011a; Tao et al. 2014). Field blank measurements were made each month or each season at all sites.

Meteorological data

Hourly wind speed (WS), temperature (*T*), relative humidity (RH), and daily precipitation for each site for 2011–2014 were taken from Weather Underground (http://www.underground.com/). The monthly and annual WS, *T*, RH and precipitation are respectively displayed in Fig. S1 and Table S1 in the Supplementary Information (SI). Year-to-year variations in all meteorological parameters were not significant at each site (all $p>0.05$) except RH for CAU, SZ, and QZ.

Statistical analyses

One-way analysis of variance (ANOVA) and paired-sample *t* tests were used to decide the significance of the differences in annual average gas (i.e., NH_3, NO_2, and HNO_3) concentrations and annual average meteorological data among sites or years, as well as daily average $PM_{2.5}$ concentrations among seasons at each site. Pearson correlation and linear regression analyses were conducted for the water-soluble inorganic ions in $PM_{2.5}$. All statistical analyses were performed using SPSS 11.5 (SPSS Inc., Chicago, IL, USA), and significance was defined as $p<0.05$.

Results and discussion

Spatial and annual variations of NH_3, NO_2, and HNO_3

Monthly mean concentrations of NH_3, NO_2, and HNO_3 at the five sites are shown in Fig. 2. The concentrations of NH_3, NO_2, and HNO_3 across all sites were in the ranges of 1.2–42.3, 10.6–81.3, and 0.3–22.1 μg m^{-3}, respectively. Their concentrations varied greatly across sites for all measured gases. The annual mean concentrations of NH_3, NO_2, and HNO_3 at the five sites for the years between 2011 and 2014 are also presented in Fig. 2. The annual NH_3 concentrations varied from 8.5±3.7 μg m^{-3} at ZZ in 2011 to 23.7±7.2 μg m^{-3} at QZ in 2014 (Fig. 2a). The year-to-year variations in annual concentrations of NH_3 were sometimes significant at all sites except CAU and YC (details are given in Table S2). However, it is important to note that annual NH_3 levels show a slight increasing trend at the five sites. This finding is consistent with the increasing trend of NH_3 emissions during recent years in the NCP due to intensified agricultural activities (Zhang et al. 2010, 2011b). The largest annual mean NH_3 concentration was observed at QZ (16.9±5.9 μg m^{-3}), followed by YC (13.8±1.5 μg m^{-3}), CAU (13.1±1.0 μg m^{-3}), ZZ (11.1±2.0 μg m^{-3}), and SZ (10.5±1.1 μg m^{-3}) (Fig. S2). This is likely due to the fact that QZ is a typical agricultural rural site with excessive N fertilizer input (about 500–600 kg N ha^{-1} $year^{-1}$) over a large amount of agricultural land (75 % of the total land), which is the main source of NH_3 (Clarisse et al. 2009). However, the difference in the annual NH_3 concentrations during 2011–2014 across the five sites was not significant. High NH_3 concentration in urban areas is associated with NH_3 emissions from biological sources, such as humans, sewage systems, and garbage containers (Reche et al. 2002). NH_3 is a secondary pollutant in gasoline vehicle emissions that results from the reaction which occurs in the catalytic converter between NO and H (Moeckli et al. 1996). Between 2006 and 2013, the number of civil vehicles increased from 2.39 to 5.17 million in Beijing and from 0.46 to 1.72 million in Zhengzhou (CSY 2007–2014), which could result in elevated NH_3 emissions. In addition, large cities in China (e.g., Beijing and Zhengzhou) can receive large amount of agricultural NH_3 from the suburban areas (Gu et al. 2014; Xu et al. 2014). In the present study, annual NH_3 concentrations at the five sites were 4~11 times higher than the annual background atmospheric NH_3 in North China (ca. 2.1 μg m^{-3}) reported by Meng et al. (2010). NH_3 levels at different urban, suburban, and rural sites in the world are listed in Table S3.

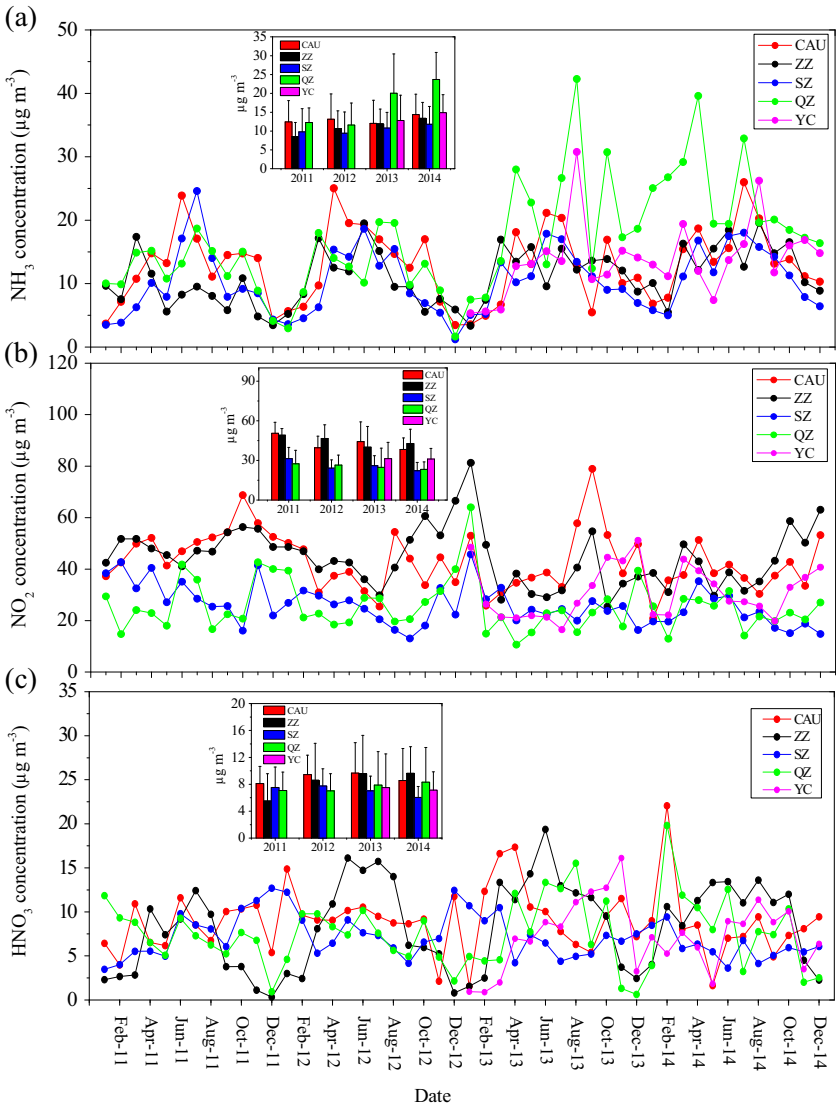

Fig. 2 Time series of monthly average concentrations of **a** NH_3, **b** NO_2, and **c** HNO_3 at the five sampling sites during 2011–2014. The annual average concentrations for the gases are shown in the *boxes inside the corresponding figures*

The average concentrations of NH_3 measured at the rural and urban sites in this study were far higher than those reported in southern China (e.g., Yang et al. 2010; Shen et al. 2013) and in other countries (e.g., Walker et al. 2004; Trebs et al. 2006; Endo et al. 2011) but were comparable to previous measurements in the NCP (e.g., Meng et al. 2011; Luo et al. 2013). NH_3 concentrations at the suburban site (SZ) were close to those observed at suburban sites with serious NH_3 pollution worldwide (Singh et al. 2001; Alebic-Juretic 2008; Cao et al. 2009). Our findings suggest that the NCP is still experiencing serious NH_3 pollution in present-day China, which is closely related to the high NH_3 emissions from N fertilizer application, intensive livestock production facilities, and high population density. For example, typical application rates of N fertilizer are 500–600 kg N ha^{-1} $year^{-1}$ for high yields of maize and wheat in rural and suburb areas. However, less than 30 % of the N fertilizer applied is taken up by the crops and more than 20 % (ca. 100 kg N ha^{-1} $year^{-1}$) is lost by NH_3 emissions (Pan et al. 2012). This makes a significant contribution to high NH_3 concentrations in the whole region. Moreover, North China is witnessing a rapid increase in livestock production facilities in suburban areas. Populations of the main livestock (pig and cattle) have increased at an annual rate of 2 % from 1996 to 2013 in North China (CSY 1997–2014). This will also result in large emissions of NH_3.

The annual average NO_2 concentrations ranged from 22.2 ±6.2 μg m^{-3} at SZ in the suburb of Beijing in 2014 to 50.5± 8.3 μg m^{-3} at CAU in the city area in 2011 (Fig. 2b). The annual concentrations at each site varied to a different extent among the years and overall exhibited a decreasing trend during the period 2011–2014 (Fig. 2b and Table S2). This finding is in accordance with the modeling results of Wang et al. (2014b) who calculated that ambient NO_2 concentration will decrease by 8 % during the 12th Five-Year Plan period (2011–2015) as a consequence of national NO_x control policies (e.g., new emission standards for power plants and vehicles). It is

interesting to observe that the year-to-year variation exhibited the same characteristic at CAU and SZ, i.e., monthly mean values were significantly lower ($p<0.05$) in 2014 than in 2011 but were not significantly different ($p>0.05$) between other years (Table S2). This result suggests that NO_2 produced in the area of the urban site can greatly affect NO_2 concentration at the suburban site. As for inter-site comparisons, annual NO_2 concentrations at the urban sites (CAU and ZZ, average 43.9± 1.0 μg m^{-3}) were significantly higher ($p<0.05$) than those at the rural and suburban sites (QZ, YC, and SZ, average 27.5± 3.2 μg m^{-3}). Differences in annual average values between the suburban and rural sites were not significant ($p>0.05$) (Fig. S2). It is commonly accepted that NO_2 is a ubiquitous air pollutant in urban regions derived mainly from fossil fuel combustion processes including power plants, transportation, and industry (Streets et al. 2003). The background concentration of atmospheric NO_2 was only about 3.7 μg m^{-3} in North China (Meng et al. 2010). In the present study, annual NO_2 concentrations at the rural sites (23.2–31.4 μg m^{-3}) were lower than those obtained in a rural area with serious NO_2 pollution in eastern China (average 42 μg m^{-3}) (Yang et al. 2010) but were much greater than those obtained in the studies of Aas et al. (2007) and Shen et al. (2013) at several rural sites in south China (Table S3), and exceed (or are close to) the annual mean NO_2 guideline value of 30 μg m^{-3} set by the World Health Organization (WHO 2000). Annual NO_2 concentrations at the urban sites (38.3–50.5 μg m^{-3}) exceeded the WHO guideline and mostly exceeded the Chinese annual exposure limit for humans of 40 μg m^{-3} for NO_2 (MEPC 2012). Compared to urban sites in other studies (Table S3), the urban NO_2 concentrations in this study were similar to those obtained at most capital cities reported by Wang et al. (2014b) for the period of 2013–2014 in China and were higher than values reported for Thessaloniki, Greece (Anatolaki and Tsitouridou 2007). Combining these findings, we conclude that many large cities in China, and rural and suburban regions in the NCP, are suffering from serous NO_2 pollution, which mainly results from high NO_x emission from the construction of new power plants and the rapid increase of vehicle numbers. According to Wang and Hao (2012), China increased its thermal power generation by 195 % and vehicle production by 300 % during 2000–2010 and NO_x emissions from power plants and transport increased by over 100 and 200 %, respectively, over the same period. The increased NO_2 emissions from newly built large power plants in North China can even be observed by satellite (Wang et al. 2012b).

NH_3 and NO_2 are two primary reactive N species in air which mainly come from human activity. The monthly mean molar ratio of NH_3 to NO_2 were in the ranges of 0.11–1.92 at the urban sites (CAU and ZZ), 0.15–2.55 at the suburban site, and 0.11–7.38 at the rural sites (QZ and YC), with overall annual values of 0.81, 1.19, and 1.74, respectively (Fig. S3). These results indicate that the concentrations of gaseous N compounds in the air are predominantly influenced by fossil fuel combustion in urban areas and by agricultural activity in non-urban areas.

In contrast to NH_3 and NO_2, the annual mean concentrations of HNO_3 at the five sites were lower and less variable, ranging from 5.5±4.1 μg m^{-3} (at ZZ in 2011) to 9.7± 4.5 μg m^{-3} (at CAU in 2014) (Fig. 2c). The year-to-year variation in annual averages was comparatively small at each site except that ZZ and SZ showed a significant difference ($p<0.05$) in monthly mean values between 2014 and 2011 and 2012, respectively (Table S2). Annual HNO_3 concentrations were not significantly different ($p>0.05$) among the five sites, with mean values of 8.9, 8.3, 7.1, 7.6, and 7.3 μg m^{-3} at CAU, ZZ, SZ, QZ, and YC, respectively (Fig. S2). This finding is not surprising because HNO_3 is produced through many pathways in the atmosphere, including photooxidation of NO_2 with OH, reaction of NO_3 with VOC, hydrolysis of N_2O_5, and dissociation of NH_4NO_3 aerosol (Khoder 2002). The fate of HNO_3 is controlled by the reaction with NH_3, which is influenced by ambient temperature, relatively humidity, and NH_3 concentrations (Sharma et al. 2007). Therefore, the absence of significant spatial difference of HNO_3 in this study is likely linked to the differences among sites in the extent of oxidation of NO_2, the contribution from other sources, and the ratio of HNO_3 and NH_3. For example, the correlations between monthly mean concentrations of NO_2 and HNO_3 were not significant at each site except for a significantly negative correlation for ZZ (Fig. S4). Moreover, NH_3 and HNO_3 were found to be highly positively corrected at ZZ, QZ, and YC (Fig. S5), suggesting that dissociation of NH_4NO_3 is the important contributor for the ambient HNO_3. Average HNO_3 concentrations in this study were comparable to those measured at two sites in the NCP reported by Luo et al. (2013) but much higher than those observed at three sites in south China (Shen et al. 2013) and at many sites worldwide (e.g., Endo et al. 2011; Trebs et al. 2006) (Table S3). The NCP has some of the highest air pollution in China due to the large amounts of coal combustion for industry and power plants and residential heating leading to high HNO_3 concentrations from oxidation of NO_2.

Seasonal variation of gaseous NH_3, NO_2, and HNO_3

The seasonal concentrations of NH_3, NO_2, and HNO_3 are dependent on their source strength and meteorological conditions. Figure 3 shows the monthly statistics of NH_3, NO_2, and HNO_3 concentrations, averaged over the 4-year period, measured at the five sites (2-year observation at YC). NH_3 concentrations across all sites were higher in March or April, especially at the rural sites (Fig. 3(a)). This can be partly explained by the enhanced NH_3 emission from natural and agricultural sources and city garbage, caused by the abrupt temperature increase after winter (Fig. S1a); every 5 °C

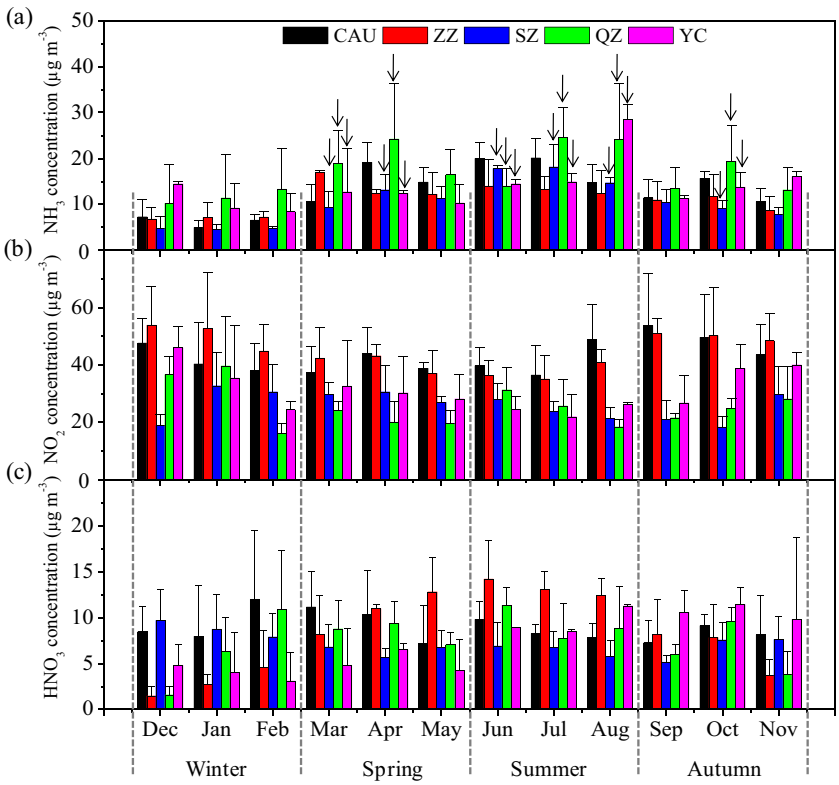

Fig. 3 The statistics of monthly average concentrations of *a* NH_3, *b* NO_2, and *c* HNO_3 during the sampling periods at the five sites. The *arrows* denote N fertilizer application for the maize-wheat crop rotation system at SZ, QZ, and YC

temperature increase nearly doubles the volatilization potential of ammonia (Sutton et al. 2013). The highest concentrations of NH_3 at all sites were in summer (June–August), which is due to the fact that high temperatures together with ammonium-N fertilizer use induce high NH_3 emissions from fertilizers. As shown in Fig. 4, NH_3 concentrations increased exponentially with the increase in air temperature at the sampling sites. The lowest concentrations of NH_3 in winter can be ascribed to the reduced NH_3 volatilization at low air temperature, high snow coverage, and infrequency of agricultural activities in winter (Cao et al. 2009). The highest NO_2 concentrations at all sites were observed in autumn (September–November) or winter (December–February) with the exception of SZ, which showed comparable values between spring and winter (Fig. 3(b)). Increased NO_2 emissions from the greater coal combustion for domestic heating (from middle November to middle March) in Northern China is the main reason for high NO_2 concentrations in autumn/winter. Moreover, agricultural crop residues in North China are not only burned as domestic fuel but are also burned directly in the field during harvest seasons (e.g., autumn), which can also cause serious local and regional NO_2 pollution (Duan et al. 2004). In addition, stable atmospheres and low temperatures appeared more frequently during autumn and winter (Fig. S1a, b), which are unfavorable meteorological conditions for air pollution dilution and dispersion (Chai et al. 2014). The lowest NO_2 concentrations were observed in summer at ZZ, SZ, and YC; in spring at QZ; and were comparable between spring and summer at CAU. In summer, stronger atmospheric mixing leads to a deeper boundary layer and a dilution of pollutants emitted from the surface, and the increased photochemistry increases the oxidation of NO_2 and its conversion rate to nitrate by reaction with OH (Yang et al. 2010). Consequently, NO_2 concentrations were lowest in summer at most sites. In contrast, the relatively high NO_2 concentration in summer at QZ and CAU is probably due to high NO_2 emissions from road traffic. The seasonal pattern of HNO_3 changes somewhat across the five sites, with the highest HNO_3 concentrations observed in winter at CAU and SZ, in summer at QZ and ZZ, and in autumn at YC (Fig. 3(c)). Different seasonal patterns of atmospheric HNO_3 in China were also reported

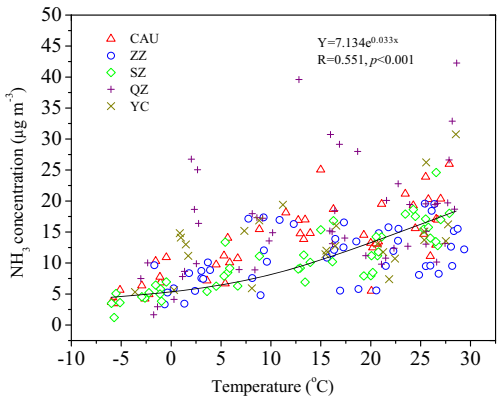

Fig. 4 Correlation between monthly average air temperature and monthly average NH_3 concentration across all five sites

in previous studies (Li et al. 2013; Luo et al. 2013; Shen et al. 2013).

Mass concentrations of $PM_{2.5}$ and water-soluble ions

Table 2 presents the summary statistics for daily average $PM_{2.5}$ concentrations during the sampling periods at the four sites. The concentrations of $PM_{2.5}$ were in the range 11.8–621.0, 19.8–692.9, 23.9–754.5, and 27.9–455.0 μg m^{-3} at CAU, SZ, QZ, and YC, respectively (data for each season per site during the sampling period are provided in Table S4). Daily average $PM_{2.5}$ concentrations were not significantly different between the sites with the exception of significantly higher $PM_{2.5}$ concentrations at CAU than at SZ. The average $PM_{2.5}$ concentration at the urban site (CAU, 159.4 μg m^{-3}) was comparable to the annual mean value of 123.5 μg m^{-3} in 2009/2010 in the urban area of Beijing (Zhao et al. 2013). Also, the average daily $PM_{2.5}$ concentration at the suburban (SZ, 141.5 μg m^{-3}) and rural (153.9 μg m^{-3} at QZ and 141.8 μg m^{-3} at YC) sites was similar to those obtained at sites with corresponding land-use types in the NCP (Shen et al. 2011). The daily average $PM_{2.5}$ concentration was a factor of 2.1 (95 % confidence interval 1.99–2.25), 1.9 (1.72–2.04), 2.1 (1.89–2.21), and 1.9 (1.75–2.03) greater than the Chinese Grade II standard for daily $PM_{2.5}$ concentration (75 μg m^{-3}, MEPC 2012) at CAU, SZ, QZ, and YC, respectively. When compared to the WHO guideline for daily $PM_{2.5}$ concentration (25 μg m^{-3}, WHO 2005), the ratios were even higher, being 6.4 (5.99–6.76) at CAU, 5.7 (5.18–6.14) at SZ, 6.2 (5.67–6.64) at QZ, and 5.7 (5.24–6.11) at YC. More than 70 % of the sampling days had daily average $PM_{2.5}$ concentration above the Chinese Grade II standard at the four sites, especially at YC (94 %). Compared with the WHO standard for daily average $PM_{2.5}$, almost all (>98 %) of the daily $PM_{2.5}$ concentration exceeded the standard. Obviously, severe $PM_{2.5}$ pollution not only existed in the urban area but also in suburban and rural areas in the NCP.

Table 2 Summary statistics for daily average $PM_{2.5}$ concentrations (μg m^{-3}) during the sampling period at the four sites

	CAU	SZ	QZ	YC
Mean	159.4	141.5	153.8	141.8
Median	137.3	110.3	126.4	127.7
Min	11.8	19.8	23.9	27.9
Max	621.0	692.9	754.5	455.0
SD	95.8	105.9	101.5	68.4
N	384	299	270	155
ECGS (%)[a]	80.5	72.6	79.6	93.5
EWHOS (%)[b]	98.2	99.7	99.6	100

N number of samples

[a] The proportion of sampling days which had concentrations of $PM_{2.5}$ exceeded the Chinese Grade II standard

[b] The proportion of sampling days which had concentrations of $PM_{2.5}$ exceeded the WHO standard

At four sites, the daily $PM_{2.5}$ concentrations during summer were lower than those in other seasons (Fig. 5). Higher rainfall in summer at all sites (Fig. S1d) promotes the scavenging of particles by wet deposition. In addition, higher temperatures during summer (Fig. S1a) favor the volatilization of fine particle nitrate to NH_3 and HNO_3 (Seinfeld and Pandis 2006). Different seasonal characteristics for highest $PM_{2.5}$ concentrations were found in the present study. At CAU, the maximum concentrations were in spring and winter, with no significant difference between the two seasons. This seasonal pattern is consistent with that for the period 2005–2008 in Beijing investigated by Yu et al. (2011) but is different from the finding of Zhao et al. (2013) who reported similar seasonal $PM_{2.5}$ concentrations across seasons in Beijing in 2009/2010, ascribed to the promotion of electricity and natural gas use. So, our result may imply that combustion of fossil fuel is still the important source of $PM_{2.5}$ in Beijing, regardless of differences in meteorological conditions (e.g., wind direction, wind speed) during experiment periods between the two studies. At QZ and SZ, the concentrations were not significantly different between spring, autumn, and winter. As revealed by Yu et al. (2011), high $PM_{2.5}$ concentrations in spring in Beijing were mainly dominated by geogenic particles from the west and northwest of China via atmospheric transport. In contrast, high concentrations of $PM_{2.5}$ in winter and autumn resulted from the combination of coal and biomass burning for domestic home heating and direct burning of agricultural residues in the field (Hu et al. 2014). Moreover, stable meteorological conditions during autumn and winter (see "Seasonal variation of gaseous NH_3, NO_2, and HNO_3") also lead to the accumulation of air pollutants. The $PM_{2.5}$ concentrations at YC were significantly higher only in winter as compared to the other three seasons, among which there was no significant difference in $PM_{2.5}$ concentration. Low $PM_{2.5}$ concentration in spring at YC is associated with a combination of fewer samples collected in the spring of 2013 (Table S4) and missing days with serious particle pollution.

The average concentrations of water-soluble ionic species during the sampling period at the four sites are presented in Table 3. The proportion of the water-soluble ions in $PM_{2.5}$ was similar for the urban site (36 %), the suburban site (34 %), and the rural sites (average 40 %). The concentrations of ions at the urban and suburban sites were both in the order $NH_4^+ > Ca^{2+} > K^+ > Na^+ > Mg^{2+}$ for the cations and $NO_3^- > SO_4^{2-} > Cl^- > F^-$ for the anions. At the rural sites, the concentration order was $NH_4^+ > K^+ > Ca^{2+} > Na^+ > Mg^{2+}$ for the cations and $SO_4^{2-} > NO_3^- > Cl^- > F^-$ for the anions. The SO_4^{2-}, NO_3^-, and NH_4^+ are the dominant ionic species, contributing 29–39 % of the average $PM_{2.5}$ mass across the four sites (Table 3). The

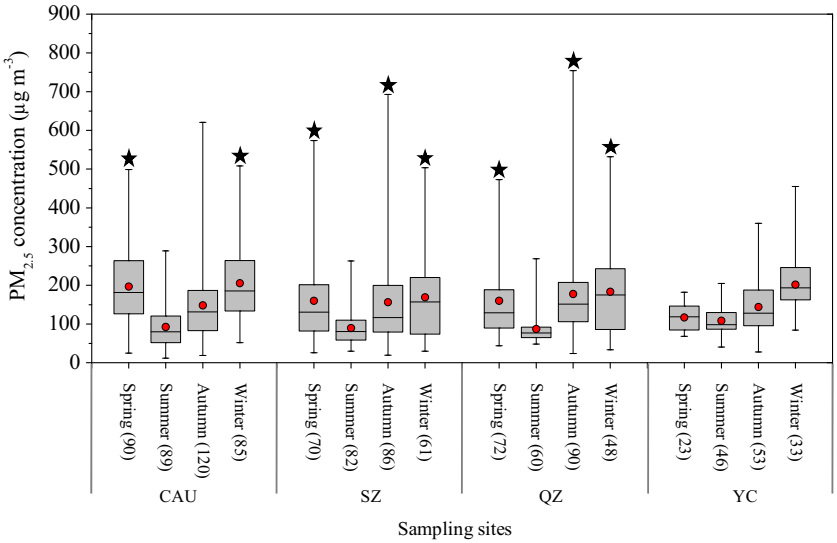

Fig. 5 Seasonal $PM_{2.5}$ concentrations at the four sites. The *box and whiskers* denote the minimum, 25th percentile, median, 75th percentile, and maximum; the *dots* denote the mean values, and those without statistical significance ($p>0.05$) among them are marked with a *star*

sampling sites in the present study were located in Beijing and its neighboring provinces (far from the ocean), where the contribution to aerosols from sea salt spray could be ignored (Yuan et al. 2004). The inconsistent order of Ca^{2+} and K^+ between non-rural and rural sites is likely due to the differences in contributions from road and soil dust and biomass burning, as the fine mode Ca^{2+} and K^+ are widely regarded as indicators of mineral dust and biomass burning, respectively (Zhao et al. 2010). The average mass ratios of NO_3^-/SO_4^{2-} were 1.15±0.90, 1.10±0.82, 0.81±0.53, and 0.81±0.49 for CAU, SZ, QZ, and YC, respectively. The higher ratios at CAU and SZ indicate a greater fraction of particles sourced from automobile exhaust. Lower NO_3^-/SO_4^{2-} ratio at QZ and YC could reflect the dominant coal combustion sources for particles.

Figure 6 illustrates the acid-base balance of the inorganic ions in $PM_{2.5}$ at the four sites. The ion balance expresses the equivalent concentration (μeq m^{-3}) of total inorganic anions (sum of NO_3^-, SO_4^{2-}, Cl^-, F^-) to cations (sum of NH_4^+, Ca^{2+}, K^+, Na^+, and Mg^{2+}). The correlation coefficients for the anion versus cation concentration data stratified by season all were greater than 0.92 at all sites, suggesting a common origin of the ions in $PM_{2.5}$. The slopes (anion/cation) of the linear regressions for all $PM_{2.5}$ samples were equal to the theoretical

Table 3 Average mass concentrations of $PM_{2.5}$ species during the sampling period at the four sites

	CAU Mean±SD	SZ Mean±SD	QZ Mean±SD	YC Mean±SD
$PM_{2.5}$ (μg m^{-3})	159.40±95.76	141.50±105.89	153.85±101.53	141.78±68.38
NO_3^- (μg m^{-3})	19.23±18.98	16.26±19.28	16.01±15.95	18.09±15.13
SO_4^{2-} (μg m^{-3})	18.61±17.92	15.21±14.80	20.08±16.06	24.52±14.66
NH_4^+ (μg m^{-3})	10.78±10.26	9.67±9.54	10.49±8.31	12.25±7.02
Cl^- (μg m^{-3})	3.74±4.82	2.28±2.70	3.52±4.36	2.42±2.81
Ca^{2+} (μg m^{-3})	2.64±1.98	1.82±1.72	1.60±1.59	1.25±1.06
Na^+ (μg m^{-3})	0.93±0.87	0.84±0.73	0.71±0.69	0.70±0.69
K^+ (μg m^{-3})	1.32±1.24	1.21±1.16	1.73±1.24	2.04±1.43
Mg^{2+} (μg m^{-3})	0.32±0.27	0.26±0.18	0.23±0.23	0.24±0.26
F^- (μg m^{-3})	0.26±0.26	0.18±0.19	0.21±0.24	0.27±0.26
Sum of ionic species (μg m^{-3})	58.84±48.88	47.73±43.78	55.31±41.95	61.97±35.63
Secondary inorganic aerosol (μg m^{-3})	48.6±44.9	41.2±40.8	46.6±37.2	54.9±33.1
WSII (%)[a]	0.35±0.18	0.34±0.17	0.35±0.15	0.44±0.15
SIA (%)[b]	0.29±0.17	0.29±0.16	0.30±0.14	0.39±0.15

[a] Proportion of water-soluble inorganic ions in $PM_{2.5}$

[b] Proportion of secondary inorganic ions in $PM_{2.5}$

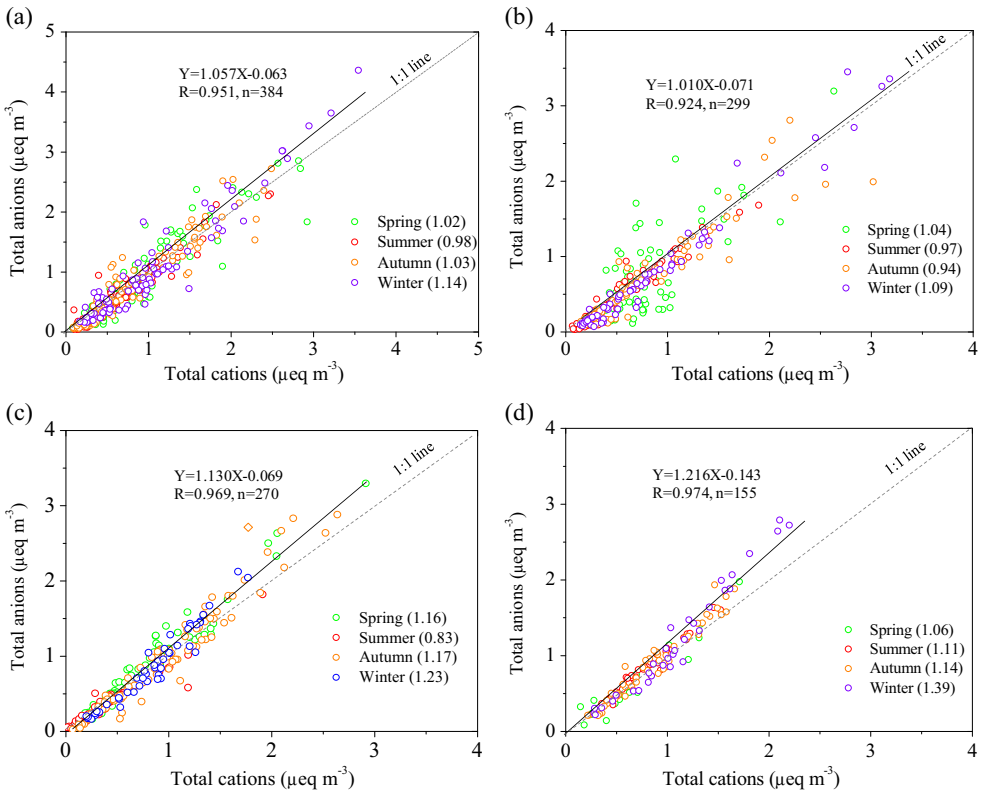

Fig. 6 The molar inorganic ion balance in $PM_{2.5}$ at the four sites: **a** CAU, **b** SZ, **c** QZ, and **d** YC

equivalent ratio of 1 at CAU (1.06) and SZ (1.01) but were greater than 1.1 at QZ (1.13) and YC (1.22). These results imply that the aerosols were neutral at the urban and suburban sites but acidic at the rural sites. The acidic $PM_{2.5}$ observed at the rural sites is most likely due to relatively low concentrations of Ca^{2+} which play an important role in spatial distribution of $PM_{2.5}$ acidity (He et al. 2012). Fully neutralized aerosol have been widely observed in different areas worldwide (Shon et al. 2012; Tao et al. 2014), but acidic aerosol has also been reported by many previous studies (Wang et al. 2006; Zhang et al. 2011a; He et al. 2012). The seasonal anion/cation ratios at the four sites, i.e., the slopes of linear regressions for the seasonally stratified data, were found to vary moderately (Fig. 6). This characteristic is consistent with the findings of Shon et al. (2012), who suggested that seasonal variation in ratio of anion/cation was caused by unmeasured cations such as ferric and non-ferric components.

Secondary inorganic aerosol

Ammonia in the atmosphere can react with H_2SO_4 to form ammonium sulfate ($(NH_4)_2SO_4$) and ammonium bisulfate (NH_4HSO_4) and react with HNO_3 and HCl to form ammonium nitrate (NH_4NO_3) and ammonium chloride (NH_4Cl) (Ianniello et al. 2010). These compounds are referred to as "secondary inorganic aerosol (SIA)" in this paper. The 4Pearson correlation coefficients between the molar concentrations of NO_3^-, SO_4^{2-}, and Cl^- in $PM_{2.5}$ are presented in Table S5. At the four sites, the correlation coefficients (CCs) between NH_4^+, SO_4^{2-}, and NO_3^- were comparable, but both of them were higher than CCs between NH_4^+ and Cl^-. Moreover, the CCs between NH_4^+ and the sum of NO_3^- and SO_4^{2-} at all sites (except SZ) were higher than those between NH_4^+ and the sum of NO_3^-, SO_4^{2-}, and Cl^-. These results mean NH_4^+ was probably mainly combined with NO_3^- and SO_4^{2-}. In order to further understand the neutralization processes between them, we calculated the molar concentrations of positive electric charges of NH_4^+ (PEC=NH_4^+/18) and negative electric charges of NO_3^- and SO_4^{2-} (NEC=NO_3^-/62+$2\times SO_4^{2-}$/96). If all sulfate was assumed to be in the form of HSO_4^-, then NEC=(NO_3^-/62+SO_4^{2-}/96) (Louie et al. 2005; Zhao et al. 2013). The seasonal average PEC and NEC are shown in Fig. 7. At all sites, we found that NH_4^+ was enough to match NO_3^- and SO_4^{2-} to form NH_4HSO_4 in all four seasons and not sufficient to meet the complete neutralization of SO_4^{2-} and NO_3^- for formation of $(NH_4)_2SO_4$ aerosol in most seasons. This indicates acid-rich conditions at the study sites. Interestingly, our findings at CAU differ from results for urban sites in Beijing and its surrounding provinces during 2009–2010 when NH_4^+ concentrations were far from enough to match NO_3^- and SO_4^{2-} throughout the year (Zhao et al. 2013). We can infer the enhanced alkalization of the atmosphere in Beijing and/or its surrounding areas because the levels of NO_3^- and SO_4^{2-} were closely comparable between

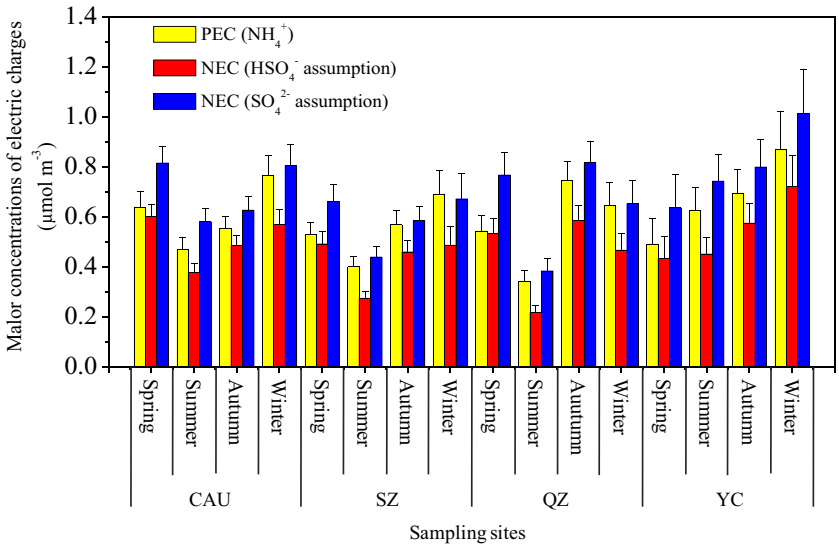

Fig. 7 Molar concentrations of positive electric charges of NH_4^+ (PEC) and negative electric charges of NO_3^- and SO_4^{2-} (NEC)

the two studies. The average molar ratio of NH_4^+ to SO_4^{2-} were 3.07±2.08 at CAU, 3.96±2.53 at SZ, 2.84±1.23 at QZ, and 2.85±0.97 at YC, suggesting the main form of $(NH_4)_2SO_4$. According to Guo et al. (2014), reductions in emissions of the aerosol precursor gases from transportation and industry are essential to mediate severe haze pollution in China. Based on our findings, we suggest that a feasible and ideal pathway to control $PM_{2.5}$ pollution in the NCP should target ammonia and acid gases together.

The average SIA concentrations (the sum of NO_3^-, SO_4^{2-}, and NH_4^+) were 48.6±44.9, 41.2±40.8, 46.6±37.2, and 54.9 ±33.1 μg m^{-3} at CAU, SZ, QZ, and YC, respectively (Table 3). All averages exceeded the Chinese ambient air quality standard for annual average value of $PM_{2.5}$ (grade II, 35 μg m^{-3}) (MEPC 2012), suggesting serious SIA pollution at all sites. The SIA concentrations in the present study were much higher than those reported in many European countries, the USA, and other developed countries (Shen et al. 2013), as well as many other cities in China (Zhang et al. 2011a). SIA concentrations at CAU were comparable to values in urban Beijing reported by a recent study (Zhao et al. 2013) but were obviously higher than 2001–2003 observations at five urban sites in Beijing (average 35.9 μg m^{-3}, Wang et al. 2005). This reflects enhanced emissions of the gaseous precursors (i.e., NH_3, SO_2, and NO_x) as a result of substantial increase in vehicle traffic, coal consumption, etc.

Seasonal concentrations of SIA at the four sites are shown in Fig. 8. At all sites except YC, the seasonal pattern of SIA is similar to that of $PM_{2.5}$ (Fig. 5), consistent with the findings of Yin et al. (2014). The SO_4^{2-} concentrations at the urban and suburban sites (CAU and SZ) exhibited a consistent seasonal variation, with the order ranked by winter>spring>summer> autumn (Fig. 8). It should be noted that the average SO_4^{2-} concentration in winter (22.7 μg m^{-3}) at CAU was slightly higher than the concentration (19.1 μg m^{-3}) observed in Beijing for winter in 2009 (Zhao et al. 2013). The similar level of sulfate loading suggests that the effect of gas desulfurization in power plants might be greatly offset by the increasing coal consumption. In contrast, the seasonal SO_4^{2-} concentrations at the rural sites were ranked in different orders: spring, autumn>winter>summer at QZ and summer, winter>autumn>spring at YC. We observed relatively high SO_4^{2-} concentrations in summer at each site. However, SO_2 concentrations were usually lowest in summer (Table S6) not only because of lower coal combustion but also owing to the increased photochemical oxidation activity, which was one of the important factors for the enhanced sulfate level in summer (Husain and Dutkiewicz 1990). At all sites, NO_3^- concentrations were distinctly lower in summer than in the other three seasons (Fig. 8). Nitrate is more sensitive to temperature, and higher temperature in summer does not favor the formation of nitrate. Moreover, a large portion of ammonium nitrate (NH_4NO_3) could evaporate from the filters, especially in

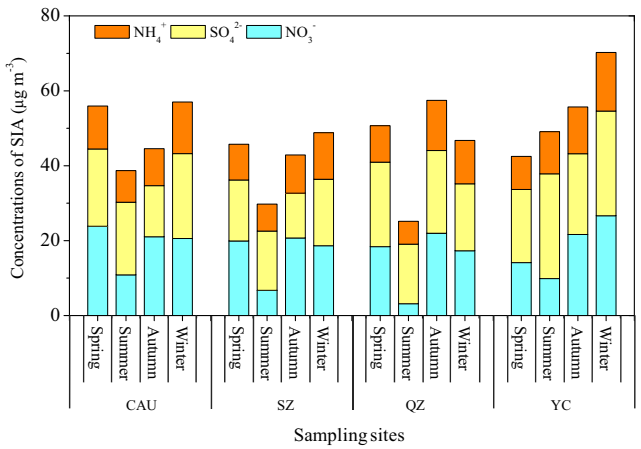

Fig. 8 Average seasonal concentrations of secondary inorganic aerosol at the four sites

summer (Ianniello et al. 2011). In contrast, low temperature and high emissions of NO_x were favorable for formation of NO_3^- aerosol and the reaction with NH_4^+ (Mariani and Mello 2007). As already discussed in "Seasonal variation of gaseous NH_3, NO_2, and HNO_3," NO_x emissions increase between mid-September and mid-March which, in combination with winter heating under relatively low temperature during that period (Fig. S1a), lead to high NO_3^- concentrations. NH_4^+ concentrations at the four sites were higher in autumn and winter than in spring and summer. The formation of NH_4^+ depends on air concentrations of acid gases, temperature, water availability (Khoder 2002), as well as flux rates of NH_3 (Nemitz et al. 2001). Compared with spring and summer, the lower temperature and higher SO_2 and NO_x emissions in winter and autumn, especially in winter, favor the gas-to-particle phase conversion and result in higher NH_4^+ aerosol concentration. Previous studies also showed higher NH_4^+ in winter compared with higher NH_3 in summer (Shen et al. 2009; Zhang et al. 2011a; Li et al. 2012).

Summary and conclusions

This study provides insights into the characteristics of variations in atmospheric pollutants over three typical land-use types in the North China Plain during China's 12th FYP (2011–2015) period, which targeted the reduction of national NO_x emissions, as well as SO_2 and primary particles. The major results and conclusions are as follows:

1. Atmospheric NH_3 concentrations showed clear spatial variation among the five sites. However, it was found that the difference in annual NH_3 concentrations was not significant across all sites. High NH_3 concentration observed at the urban site was probably due to high emissions from biological sources (e.g., sewage systems and garbage containers) and vehicles in the urban area, as well as agricultural activity in the suburban area. Annual average NH_3 concentrations showed consistent increasing trends at the five sites, reflecting the elevated NH_3 emission intensities from transportation, agriculture, and livestock husbandry.
2. Annual average NO_2 concentrations exhibited obvious spatial difference, showing significantly higher concentrations at the urban site than at the suburban and rural sites. An overall decreasing trend of annual NO_2 concentrations was observed at all sites, likely related to implementation of the national controls on NO_x emissions. All annual averages, however, exceeded (or were close to) the Chinese annual NO_2 exposure limit for humans, indicating serious atmospheric NO_2 pollution not only at the urban site but also at suburban and rural sites resulting from local emission sources and atmospheric transport.
3. Unlike for NH_3 and NO_2, annual average HNO_3 concentrations were relatively low and showed small spatial and annual variations.
4. The $PM_{2.5}$ pollution was severe in the NCP, with more than 70 % of sampling days across the sites exceeding the Chinese Grade II standard for daily $PM_{2.5}$ concentration. Ion balance calculations indicated that $PM_{2.5}$ was neutral at the urban and suburban sites and acidic at the rural sites.
5. NO_3^-, SO_4^{2-}, and NH_4^+ were the dominant ionic particulate species at the four sites and accounted for 29–39 % of the $PM_{2.5}$ mass. NH_4^+ was the dominant cation at all sites, whereas NO_3^- and SO_4^{2-} were the dominant anions at the non-rural and rural sites, respectively. NH_4^+ was insufficient to fully neutralize SO_4^{2-} and NO_3^- at all sites, indicating an acid-rich condition. The seasonal variation of SIA was similar to that of $PM_{2.5}$, implying that a reduction of the concentrations of SIA is a feasible way to control $PM_{2.5}$ pollution in the NCP, by directly targeting ammonia or/and acid gases. Compared with observations of the three dominant ions in Beijing in previous studies, enhanced alkalization of the atmosphere was found.
6. Similar seasonal variations were observed for concentrations of NH_3, NO_2, and aerosols NO_3^- and NH_4^+ over the three land-use types, whereas seasonal variation of $PM_{2.5}$ and HNO_3 concentrations showed different spatial characteristics. All above seasonal patterns were affected by meteorological condition and pollution sources.

Acknowledgments The study was supported by the China National Fund for Distinguished Young Scientists (Grant 40425007) and the innovative group grant of NSFC (Grant 31421092). We thank Ms. Lu Li and Zhao Jingxian for their help in collecting and analyzing samples.

References

Aas W, Shao M, Jin L, Larssen T, Zhao DW, Xiang RJ et al (2007) Air concentrations and wet deposition of major inorganic ions at five non-urban sites in China, 2001–2003. Atmos Environ 41:1706–1716

Alebic-Juretic A (2008) Airborne ammonia and ammonium within the Northern Adriatic area, Croatia. Environ Pollut 154:439–447

Allegrini I, De Santis F, Di Palo V, Febo A, Perrino C, Possanzini M (1987) Annular denuder method for sampling reactive gases and aerosols in the atmosphere. Sci Total Environ 67:1–16

Anatolaki C, Tsitouridou R (2007) Atmospheric deposition of nitrogen, sulfur and chloride in Thessaloniki, Greece. Atmos Res 91:413–428

Cao JJ, Zhang T, Chow JC, Watson JG, Wu F, Li H (2009) Characterization of atmospheric ammonia over Xi'an, China. Aerosol Air Qual Res 9:277–289

Chai FH, Gao J, Chen ZX, Wang SL, Zhang YC, Zhang JQ et al (2014) Spatial and temporal variation of particulate matter and gaseous pollutants in 26 cities in China. J Environ Sci 26:75–82

Clarisse L, Clerbaux C, Dentener F, Hurtmans D, Coheur PF (2009) Global ammonia distribution derived from infrared satellite observations. Nat Geosci 2:479–483

CSY (1997–2014) China Statistics Yearbook. Available at:http://www.stats.gov.cn

CSY (2007–2014) China Statistics Yearbook. Available at:http://www.stats.gov.cn

CSY (2014) China Statistical Yearbook. Available at:http://www.stats.gov.cn

Dominici F, Greestone M, Sunstein CR (2014) Particulate matter matters. Science 344:257–259

Duan F, Liu X, Yu T, Cachier H (2004) Identification and estimate of biomass burning contribution to the urban aerosol organic carbon concentrations in Beijing. Atmos Environ 38:1275–1282

Endo T, Yagoh H, Sato K, Matsuda K, Hayashi K, Noguchi I et al (2011) Regional characteristics of dry deposition of sulfur and nitrogen compounds at EANET sites in Japan from 2003 to 2008. Atmos Environ 45:1259–1267

Flechard CR, Nemitz E, Smith RI, Fowler D, Vermeulen AT, Bleeker A et al (2011) Dry deposition of reactive nitrogen to European ecosystems: a comparison of inferential models across the NitroEurope network. Atmos Chem Phys 11:2703–2728

Gu BJ, Ge Y, Ren Y, Xu B, Luo WD, Jiang H et al (2012) Atmospheric reactive nitrogen in China: sources, recent trends, and damage costs. Environ Sci Technol 46:9240–9247

Gu BJ, Sutton MA, Chang SX, Ge Y, Jie C (2014) Agricultural ammonia emissions contribute to China's urban air pollution. Front Ecol Environ 12:265–266

Guo YM, Jia YP, Pan XC, Liu LQ, Wichmann HE (2009) The association between fine particulate air pollution and hospital emergency room visits for cardiovascular diseases in Beijing, China. Sci Total Environ 407:4826–4830

Guo S, Hu M, Zamora ML, Peng JF, Shang DJ, Zheng J et al (2014) Elucidating severe urban haze formation in China. Proc Natl Acad Sci U S A 111:17373–17378

He K, Zhao Q, Ma Y, Duan F, Yang F, Shi Z et al (2012) Spatial and seasonal variability of $PM_{2.5}$ acidity at two Chinese mega cities: insights into the formation of secondary inorganic aerosols. Atmos Chem Phys 12:1377–1395

Hu J, Wang Y, Ying Q, Zhang H (2014) Spatial and temporal variability of $PM_{2.5}$ and PM_{10} over the North China Plain and the Yangtze River Delta, China. Atmos Environ 95:598–609

Huang X, Song Y, Li MM, Li JF, Huo Q, Cai XH et al (2012) A high-resolution ammonia emission inventory in China. Global Biogeochem Cy 26:GB1030

Husain L, Dutkiewicz VA (1990) A long term (1975–1988) study of atmospheric SO_4^{2-}: regional contributions and concentration trends. Atmos Environ 24A:1175–1187

Ianniello A, Spataro F, Esposito G, Allegrini I, Rantica E, Ancora MP et al (2010) Occurrence of gas phase ammonia in the area of Beijing (China). Atmos Chem Phys 10:9487–9503

Ianniello A, Spataro F, Esposito G, Allegrini I, Hu M, Zhu T (2011) Chemical characteristics of inorganic ammonium salts in $PM_{2.5}$ in the atmosphere of Beijing (China). Atmos Chem Phys 11:10803–10822

Khoder MI (2002) Atmospheric conversion of sulfur dioxide to particulate sulfate and nitrogen dioxide to particulate nitrate and gaseous nitric acid in an urban area. Chemosphere 49:675–684

Li KH, Song W, Liu XJ, Zhang W, Shen JL, Liu B et al (2012) Atmospheric reactive nitrogen concentrations at ten sites with contrasting land use in an arid region of central Asia. Biogeosciences 9:4013–4021

Li KH, Liu XJ, Song W, Chang YH, Hu YK, Tian CY (2013) Atmospheric nitrogen deposition at two sites in an arid environment of central Asia. PLoS ONE 8:e67018

Louie PKK, Chow JC, Antony Chen LW, Watson JG, Leung G, Sin DWM (2005) $PM_{2.5}$ chemical composition in Hong Kong: urban and regional variations. Sci Total Environ 338:267–281

Luo XS, Liu P, Tang AH, Liu JY, Zong XY, Zhang Q et al (2013) An evaluation of atmospheric N_r pollution and deposition in North China after the Beijing Olympics. Atmos Environ 74:209–216

Mariani RL, Mello WZD (2007) $PM_{2.5-10}$, $PM_{2.5}$ and associated water-soluble inorganic species at a coastal urban site in the metropolitan region of Rio de Janeiro. Atmos Environ 41:2887–2892

Meng ZY, Xu XB, Wang T, Zhang XY, Yu XL, Wang SF et al (2010) Ambient sulfur dioxide, nitrogen dioxide, and ammonia at ten background and rural sites in China during 2007–2008. Atmos Environ 44:2625–2631

Meng ZY, Lin WL, Jiang XM, Yan P, Wang Y, Zhang YM et al (2011) Characteristics of atmospheric ammonia over Beijing, China. Atmos Chem Phys 11:6139–6151

MEPC (2011) Ministry of Environment Protection of China. Report on environmental quality in China, 2010. Available at: http://www.mep.gov.cn/ (accessed January 2011)

MEPC (2012) Ministry of Environment Protection of China. Ambient air quality standards (GB3095–2012). Available at: http://www.mep.gov.cn/ (accessed 29 February 2012)

Moeckli MA, Fierz M, Sigrist MW (1996) Emission factors for ethane and ammonia from a tunnel study with a photoacoustic trace gas detection system. Environ Sci Technol 30:2864–2867

Nemitz E, Milford C, Sutton MA (2001) A two-layer canopy compensation point model for describing bi-directional biosphere–atmosphere exchange of ammonia. Q J Roy Meteor Soc 127:815–833

Pan YP, Wang YS, Tang GQ, Wu D (2012) Wet and dry deposition of atmospheric nitrogen at ten sites in Northern China. Atmos Chem Phys 12:6515–6535

Perrino C, Gherardi M (1999) Optimization of the coating layer for the measurement of ammonia by diffusion denuders. Atmos Environ 33:4579–4587

Perrino C, De Santis F, Febo A (1990) Criteria for the choice of a denuder sampling technique devoted to the measurement of atmospheric nitrous and nitric acids. Atmos Environ 24A:617–626

Reche C, Viana M, Pandolfi M, Alastuey A, Moreno T, Amato F et al (2002) Urban NH_3 levels and sources in a Mediterranean environment. Atmos Environ 57:153–164

Seinfeld J, Pandis S (2006) Atmospheric chemistry and physics: from air pollution to climate change, John Wiley and Sons, 2nd Edition, pp1203

Sharma M, Kishore S, Tripathi SN, Behera SN (2007) Role of atmospheric ammonia in the formation of inorganic secondary particulate matter: a study at Kanpur, India. J Atmos Chem 58:1–17

Shen JL, Tang AH, Liu XJ, Fangmeier A, Goulding KTW, Zhang FS (2009) High concentrations and dry deposition of reactive nitrogen species at two sites in the North China Plain. Environ Pollut 157:3106–3113

Shen JL, Liu XJ, Fangmeier A, Goulding K, Zhang FS (2011) Atmospheric ammonia and particulate ammonium from agricultural sources in the North China Plain. Atmos Environ 45:5033–5041

Shen JL, Li Y, Liu XJ, Luo XS, Tang AH, Zhang YZ et al (2013) Atmospheric dry and wet nitrogen deposition on three contrasting land use types of an agricultural catchment in subtropical central China. Atmos Environ 67:415–424

Shon ZH, Kim KH, Song SK, Jung K, Kim NJ, Lee JB (2012) Relationship between water-soluble ions in $PM_{2.5}$ and their precursor gases in Seoul megacity. Atmos Environ 59:540–550

Singh SP, Satsangi GS, Khare P, Lakhani A, Maharaj KK et al (2001) Multiphase measurement of atmospheric ammonia. Chemosphere Global Change Sci 3:107–116

Song Y, Zhang YH, Xie SD, Zeng LM, Zheng M, Salmon LG et al (2006) Source apportionment of $PM_{2.5}$ in Beijing by positive matrix factorization. Atmos Environ 40:1526–1537

Spataro F, Ianniello A, Esposito G, Allegrini I, Zhu T, Hu M (2013) Occurrence of atmospheric nitrous acid in the urban area of Beijing (China). Sci Total Environ 447:210–224

Streets DG, Bond TC, Carmichael GR, Fernandes SD, Fu Q, He D et al (2003) An inventory of gaseous and primary aerosol emissions in Asia in the year 2000. J Geophys Res 108:8809

Sun YL, Zhuang GS, Wang Y, Han LH, Guo JH, Dan M et al (2004) The air-borne particulate pollution in Beijing-concentration, composition, distribution and sources. Atmos Environ 38:5991–6004

Sun YL, Zhuang GS, Tang AH, Wang Y, An ZS (2006) Chemical characteristics of $PM_{2.5}$ and PM_{10} in haze-fog episodes in Beijing. Environ Sci Technol 40:3148–3155

Sutton MA, Reis S, Riddick SN, Dragosits U, Nemitz E, Theobald MR et al (2013) Towards a climate-dependent paradigm of ammonia emission and deposition. Philo T R Soc B 368:20130166

Tang YS, Simmons I, van Dijk N, Di Marco C, Nemitz E, Dammgen U et al (2009) European scale application of atmospheric reactive nitrogen measurements in a low-cost approach to infer dry deposition fluxes. Agr Ecosyst Environ 133:183–195

Tao Y, Yin Z, Ye XN, Ma Z, Che JM (2014) Size distribution of water-soluble inorganic ions in urban aerosols in Shanghai. Atmos Pollut Res 5:639–647

Trebs I, Lara LL, Zeri LMM, Gatti LV, Artaxo P, Dlugi R et al (2006) Dry and wet deposition of inorganic nitrogen compounds to a tropical pasture site (Rondônia, Brazil). Atmos Chem Phys 6:447–469

Walker JT, Whitall D, Robarge WP, Paerl H (2004) Ambient ammonia and ammonium aerosol across a region of variable ammonia emission density. Atmos Environ 38:1235–1246

Wang SX, Hao JM (2012) Air quality management in China: issues, challenges, and options. J Environ Sci 24:2–13

Wang Y, Zhuang GS, Tang A, Yuan H, Sun Y, Chen S et al (2005) The ion chemistry and the source of $PM_{2.5}$ aerosol in Beijing. Atmos Environ 39:3771–3784

Wang Y, Zhuang GS, Zhang XY, Huang K, Xu C, Tang AH et al (2006) The ion chemistry, seasonal cycle, and sources of $PM_{2.5}$ and TSP aerosol in Shanghai. Atmos Environ 40:2935–2952

Wang X, Ding X, Fu X, He Q, Wang S, Bernard F et al (2012a) Aerosol scattering coefficients and major chemical compositions of fine particles observed at a rural site in the central Pearl River Delta, South China. J Environ Sci 24:72–77

Wang SW, Zhang Q, Streets DG, He KB, Martin RV, Lamsal LN et al (2012b) Growth in NO_x emissions from power plants in China: bottom-up estimates and satellite observations. Atmos Chem Phys 12:4429–4447

Wang SX, Xing J, Zhao B, Jang C, Hao JM (2014a) Effectiveness of national air pollution control policies on the air quality in metropolitan areas of China. J Environ Sci 26:13–22

Wang YG, Ying Q, Hu JL, Zhang HL (2014b) Spatial and temporal variations of six criteria air pollutants in 31 provincial capital cities in China during 2013–2014. Environ Int 73:413–422

Watson JG (2002) Visibility: science and regulation. J Air Waste Manage 52:628–713

WB (2007) World Bank (WB), State Environmental Protection Administration, P.R. China. Cost of pollution in China. Economic estimates of physical damages. Available at www.worldbank.org/eapenvironment (accessed May 2013)

WHO (2000) World Health Organization (WHO), Air Quality Guidelines for Europe, WHO Regional Office for Europe. WHO Regional Publications, European Series No. 91, Copenhagen

WHO (2005) World Health Organization (WHO), WHO air quality guidelines for particulate matter, ozone, nitrogen dioxide and sulfur dioxide. Global Update. Summary of Risk Assessment. Geneva, Switzerland

Wu SW, Deng FR, Niu J, Huang QS, Liu YC, Guo XB (2010) Association of heart rate variability in taxi drivers with marked changes in particulate air pollution in Beijing in 2008. Environ Health Persp 118:87–91

Xu W, Zheng K, Liu XJ, Meng LM, Huaitalla RM, Shen JL et al (2014) Atmospheric NH_3 dynamics at a typical pig farm in China and their implications. Atmos Pollut Res 5:455–463

Yang R, Hayashi K, Zhu B, Li F, Yan X (2010) Atmospheric NH_3 and NO_2 concentration and nitrogen deposition in an agricultural catchment of Eastern China. Sci Total Environ 408:4624–4632

Yin LQ, Niu ZC, Chen XQ, Chen JS, Zhang FW, Xu LL (2014) Characteristics of water-soluble inorganic ions in $PM_{2.5}$ and $PM_{2.5-10}$ in the coastal urban agglomeration along the Western Taiwan Strait Region, China. Environ Sci Pollut Res 21:5141–5156

Yu Y, Schleicher N, Norra S, Fricker M, Dietze V, Kaminski U et al (2011) Dynamics and origin of $PM_{2.5}$ during a three-year sampling period in Beijing, China. J Environ Monitor 13:334–336

Yuan CS, Sau CC, Chen MC (2004) Influence of Asian dusts on the physiochemical properties of atmospheric aerosols in Taiwan district using the Penchuis lands as an example. China Particuology 2:144–152

Zhang J, Smith K (2007) Household air pollution from coal and biomass fuels in China: measurements, health impacts, and interventions. Environ Health Persp 115:848–855

Zhang Q, Streets DG, Carmichael GR, He KB, Huo H, Kannari A et al (2009) Asian emissions in 2006 for the NASA INTEX-B mission. Atmos Chem Phys 9:5131–5153

Zhang Y, Dore AJ, Ma L, Liu XJ, Ma WQ, Cape JN et al (2010) Agricultural ammonia emissions inventory and spatial distribution in the North China Plain. Environ Pollut 158:490–501

Zhang T, Cao JJ, Tie XX, Shen ZX, Liu SX, Ding H et al (2011a) Water-soluble ions in atmospheric aerosols measured in Xi'an, China: seasonal variations and sources. Atmos Res 102:110–119

Zhang Y, Dore AJ, Liu X, Zhang F (2011b) Simulation of nitrogen deposition in the North China Plain by the FRAME model. Biogeosciences 8:3319–3329

Zhao Q, He K, Rahn KA, Ma Y, Jia Y, Yang F et al (2010) Dust storms come to Central and Southwestern China, too: implications from a major dust event in Chongqing. Atmos Chem Phys 10:2615–2630

Zhao PS, Dong F, He D, Zhao XJ, Zhang XL, Zhang WZ, Yao Q, Liu HY (2013) Characteristics of concentrations and chemical compositions for $PM_{2.5}$ in the region of Beijing, Tianjin, and Hebei, China. Atmos Chem Phys 13:4631–4644